

---

# Enhanced neurite alignment on micro-patterned poly-L-lactic acid films

---

Jianming Li,<sup>1,2</sup> Helen McNally,<sup>2</sup> Riyi Shi<sup>1,2,3</sup>

<sup>1</sup>Weldon School of Biomedical Engineering, School of Veterinary Medicine, Purdue University, West Lafayette, Indiana 47907

<sup>2</sup>Center for Paralysis Research, School of Veterinary Medicine, Purdue University, West Lafayette, Indiana 47907

<sup>3</sup>Department of Basic Medical Sciences, School of Veterinary Medicine, Purdue University, West Lafayette, Indiana 47907

Received 22 November 2006; revised 9 March 2007; accepted 22 June 2007

Published online 9 January 2008 in Wiley InterScience (www.interscience.wiley.com). DOI: 10.1002/jbm.a.31814

**Abstract:** The ability of the damaged central nervous system and peripheral nervous system to properly recover hinges on the regenerative mechanisms and functional reconnection to appropriate targets. Successful pathfinding of axons is controlled by a complex interplay of diffusible or substrate-bound biochemical and electrical cues. Physical guidance has also been shown to occur *in vivo* and *in vitro*, either via cell–cell or cell–extracellular matrix mediated contact. In the current study, we probe the role of contact guidance in facilitating neural regeneration and pathfinding. Using soft lithographic techniques, we have created thin films of poly-L-lactic acid polymer (PLLA) possessing periodic features approaching the nanometer regime. Rat PC-12 cells and chick sympathetic neurons were subsequently cultured onto these substrates and parameters, such as neurite

emergence and orientation angle, neurite length, and neuronal architecture are characterized. Our results reveal that both PC-12 and chick sympathetic neurites can be effectively guided by unidirectional grooves as small as 100 nm in height and 1  $\mu\text{m}$  in width. Moreover, sympathetic cells produced neurites that were longer on patterned substrata than on controls. The development of novel degradable micro/nanopatterned substrates for cell study will permit more in-depth analysis of contact mediated guidance mechanisms in addition to having applications in neural and tissue engineering. © 2008 Wiley Periodicals, Inc. *J Biomed Mater Res* 87A: 392–404, 2008

**Key words:** topography; neurite alignment; regeneration; poly-L-lactic acid; soft lithography

---

## INTRODUCTION

The process of axonal pathfinding and regeneration are mediated by individual and or synergisms of stimulatory and inhibitory cues. Gradients of soluble biomolecules such as neurotrophins or surface-bound extracellular matrix (ECM) adhesion peptides have been implicated in facilitating regeneration and in the pathfinding process.<sup>1–5</sup> Other phenomena such as electric fields arising from endogenous ionic currents can additionally potentiate directionality and regeneration of neural cells.<sup>6–9</sup> Contact guidance refers to a phenomenon in which the substratum dis-

continuities create orientation in cell locomotion.<sup>10</sup> In the nervous system, contact guidance exists *in vivo* and may serve a role in development, growth, and regeneration.<sup>11–15</sup>

*In vitro*, *xenopus* spinal neurites and rat hippocampal cells respond to repeating parallel grooves via parallel or perpendicular alignment.<sup>16</sup> Rat hippocampal processes have also been patterned with silicon pillars of micron and submicron geometries.<sup>17</sup> Even basic topographic cues in the form of petri dish (glass) scratches were shown to promote growth cone steering and neurite alignment in chick DRG.<sup>18</sup> In most instances, photolithographic methods have been commonly used to generate finely patterned surfaces. Although lithographic processes can produce a gamut of geometries, photolithographic compatible materials are limited. Subsequently, prior experiments investigating contact guidance were achieved on materials not necessarily suitable for *in vivo* implantation. However, soft lithographic techniques such as casting and stamping are quite flexible and much more amenable to biomaterials processing.<sup>19</sup>

Correspondence to: R. Shi; e-mail: riyi@purdue.edu

Contract grant sponsor: The NSF Integrative Graduate Education and Research Training (IGERT) Program in Therapeutic and Diagnostic Devices; contract grant number: DGE-99-72770

Contract grant sponsor: The State of Indiana

In the current study, we utilize a solvent casting method to fabricate poly-L-lactic acid (PLLA) films with unidirectional grooves of submicron heights. The properties of the polymeric films and adherent cells were characterized with X-ray photoelectron spectroscopy (XPS), atomic force microscopy (AFM), and scanning electron microscopy (SEM). Questions of interest included how surface geometry played a role in governing neurite outgrowth, alignment, and overall cell complexity. To minimize interaction effects from other guidance cues, experiments were conducted *in vitro*, with rat PC-12 and chick sympathetic neurons as the model cell systems.

The necessity to assess neurite outgrowth on PLLA is evident since it is obvious that different biomaterials and surface chemistries can elicit varied cellular responses.<sup>20,21</sup> We presently chose PLLA polymer as the substrate due to its ubiquity in biomedical materials research and biodegradability. Furthermore, PLLA has been utilized in FDA approved products and is quite amenable to numerous processing schemes. Characterizing the neuronal cell response to surface contours approaching the nanoscale regime is essential in future applications that require guided neuronal regeneration. Fields of relevance include tissue engineering for central nervous system and peripheral nervous system as well as artificial networks. The soft lithographic methods presented may also be compatible with other polymer systems such as poly-lactic glycolic acid copolymer, poly-caprolactone, and even nonbiodegradable polydimethylsiloxane (PDMS).

## MATERIALS AND METHODS

### Substrate preparation

Patterned substrates were manufactured via a polymer casting technique. Poly-L-lactide of inherent viscosity 0.99 (Birmingham Polymers) was dissolved in chloroform (Mallinkrodt) in a 5% w/v concentration. Acetate holographic templates of 500 lines/mm and 1000 lines/mm (Edmunds Scientific) were cleaned with DI water, ethanol and a stream of compressed air. Next, 2 mL of the polymer solution was pipetted uniformly over a 4 cm × 5 cm portion of the master acetate template. The polymer solution was then evaporated in a fume hood for approximately 1 h. After 1 h, the polymer was carefully peeled from the masters. The PLLA film was then placed in a vacuum chamber and degassed for an additional 48 h at a pressure of 25 in Hg. In addition to the patterned PLLA substrates, two types of controls were used: Tissue culture polystyrene (TCPS; Falcon), and control PLLA surfaces replicated from tissue culture glassware. Following manufacture, all polymer sheets were cut to appropriate size (~2 × 2 cm<sup>2</sup>) and stored in vacuumed polyethylene bags. The solvent casting method

produced films approximately 20 μm thick when viewed with SEM.

### Cell culture

Prior to cell seeding, polymer substrates were sterilized with a 70/30% ethanol/water solution for 1 h and air dried in a sterile hood. Following sterilization, the PLLA films and TCPS dishes were treated with laminin (10 μg/mL, Sigma) for 5 h at 37°C. After incubation with laminin, the substrates were washed with PBS three times. The PLLA films were mounted within the Petri dish/well by using a thin (~0.5 to 1.0 mm) PDMS (Dow) underlayer to fix the films in place.

### PC-12

Rat PC-12 cells were cultured and primed (1 week) in Dulbecco's Modified Eagle Medium (DMEM; Gibco) supplemented with 12.5% horse serum, 2.5% fetal bovine serum, 1% penicillin streptomycin (Sigma), and 67 ng/mL nerve growth factor (NGF, Austral Biologics) in tissue culture dishes. Primed cells were removed from the tissue dishes with 1 h incubation in calcium free Krebs' solution (124 NaCl, 5 KCl, 1.2 KH<sub>2</sub>PO<sub>4</sub>, 1.3 MgSO<sub>4</sub>, 2 CaCl<sub>2</sub>, 20 glucose, 10 sodium ascorbate, and 26 NaHCO<sub>3</sub>, mM units). The Krebs' buffer solution containing detached cells was then transferred to a polypropylene test tube and centrifuged (TRIAc) at 12,000g for 5 min. The supernatant Krebs' was decanted and the residual cell pellet was gently triturated and resuspended in 4 mL of 67 ng/mL NGF supplemented DMEM solution. Cells were counted with a hemocytometer and seeded onto the polymer and TCPS substrates at a density of 1.5 × 10<sup>4</sup> cells/cm<sup>2</sup> (using 6 well plates or 35 mm petri dishes).

### Chick sympathetic neurons

Sympathetic ganglia from the sympathetic chain were dissected from embryonic day 7–8 chick embryos by conventional methods under a Nikon SMZ-2T stereoscope. The ganglia were subsequently placed in a solution of 0.25% trypsin (Sigma) and Puck's balanced saline. After 30 min incubation, the ganglia were transferred to a tube of neuron medium and dissociated with gentle trituration. Cells were counted with a hemocytometer and plated onto the substrates with neuron medium at a density of 5.2 × 10<sup>3</sup> cells/cm<sup>2</sup>. Sympathetic neurons were maintained in an incubator set at 37°C and 5% CO<sub>2</sub>. The neuron media consisted of F12 nutrient base (Gibco) supplemented with 2% horse serum, Penstrep, conalbumin, Vitamin C, and insulin (Sigma).

### Data collection and analysis

Cell measurements (Fig. 1) were made from digital images taken from a Nikon Diaphot 300 microscope in phase contrast mode and with a ×20 objective. Random

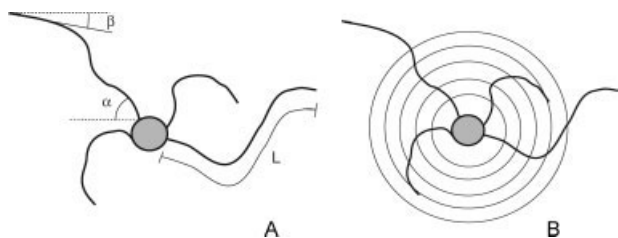


**Figure 1.** A schematic a cell and measured experimental parameters. A: The length of the neurite was found by tracing the entire process from tip to intersection with soma ( $L$ ). The neurite emergence angle ( $\alpha$ ) was the angle at which the neurite exited the cell body. The neurite orientation angle ( $\beta$ ) was found by finding the angle of the last 25–30  $\mu\text{m}$  of the neurite. Angular data was defined as the acute angle ( $<90^\circ$ ) between the neurite and a horizontal reference line. Only neurites at least 50  $\mu\text{m}$  in length were recorded. B: Analysis of neuronal architectural complexity. Five concentric circles of 37, 47, 57, 71, and 85  $\mu\text{m}$  in radius were placed over the cell body centroid. The number of intersections between neuronal processes and the circles were tabulated. Higher numbers of intersection points translate into more complex cell architecture.

fields at 24 h (chick sympathetic cells) or 48 h (PC-12 cells) after seeding were imaged with a CCD (Diagnostic Instruments). Captured grayscale images were processed and analyzed with Image Pro Plus. Only isolated cells where established neurites were clearly visible, contact-free, and greater than 50  $\mu\text{m}$  were evaluated. Neurite length measurements were made on the longest neurite branch (if branching occurred). Neurite lengths were traced manually with a cursor and calibrated to standards. Two different measurements were taken for neurite angles. The emergence angle ( $\alpha$ ) refers to the neurite exit angle from the soma while the orientation angle ( $\beta$ ) was assumed to be the articulated angle of the last 25–30  $\mu\text{m}$  of the neurite. In all cases, the direction of the substrate grooves served as the reference line (All images taken with grooves in the horizontal direction. Controls were randomly placed down and the horizontal served as the reference). Angular data was divided into  $15^\circ$  bins. Neurites were considered “parallel” if they fell between  $0\text{--}15^\circ$  of the grooves whereas perpendicular alignment was considered for  $75\text{--}90^\circ$ . Neuronal complexity was assessed using a method previously described by Sholl.<sup>22</sup> Briefly, concentric circles with radii of 37, 47, 57, 71, and 85  $\mu\text{m}$  were drawn around the cell body. The number of intersections between neuronal processes and the reference circles were counted. Lower intersection values represent a simplified architecture while higher numbers generally convey more neurites or extensive arborization.

### Atomic force microscopy

The topography of the PLLA polymer and TCPS controls were characterized using a PSIA XE-120 atomic force microscope. For mounting, PLLA polymer samples were fixed onto a PDMS (Dow) underlayer. Measurements were acquired in tapping mode using a PSIA noncontact cantilever with a spring constant of 42 N/m and a nominal tip

radius of 10 nm. The resonance frequency was 309 kHz. The original  $256 \times 256$  data point image fields were obtained at a scan rate of 1.0 Hz/line. All topography measurements were performed in air. AFM data was analyzed with XEI Software.

### X-ray photoelectron spectroscopy

A Kratos Axis Ultra with a monochromatic (Al)  $K\alpha$  X-ray source operating at 1486.69 eV was used for XPS investigation. The magnification used was  $1 \text{ e} +037$  with resolution of 160. Prior to XPS, the PLLA films were cleansed in 70/30 ethanol and air dried in a covered petri dish. Specimens were subsequently mounted onto a metal holder and placed into the XPS chamber set to  $2 \times 10^{-9}$  torr vacuum. Wide and narrow scans were acquired on control and patterned films at two distinct foci.

### Scanning electron microscopy

Polymeric films with plated cells were fixed with 2% glutaraldehyde solution in 0.1M cacodylate buffer and 1% osmium tetroxide in 0.1M cacodylate buffer. The samples were dehydrated with a series of ethanol dilutions (30, 50, and 70%) and then critical point dried. The specimens were then mounted onto aluminum disks and sputtered coated with gold-palladium. Imaging was performed on a JEOL JSM-840 SEM using a 5 kV acceleration voltage. Digital images were captured with  $1280 \times 960$  resolution and 160 s dwell time.

### Statistical treatment

Unless noted, the nonparametric Kruskal–Wallis and Dunn’s multiple comparison tests were used to assess differences between populations. For proportion evaluations, the large sample proportion procedure was employed. A  $p$ -value of  $< 0.05$  was considered to be statistically significant in all cases.

## RESULTS

### Substrate geometry

AFM confirmed the spatial periodicity of the PLLA substrates to be 1 and 2  $\mu\text{m}$  [Fig. 2(A,B)]. The cross sectional geometry of the cast polymer channels was sinusoidal, which accurately reflected the ruled holographic masters (images not shown). The replica polymer films also reproduced native surface irregularities/roughness of the original templates. These imperfections were generally  $<10$  nm in height and were much smaller than the groove height variations. Additional submicron pores tens of nanometers in height were occasionally seen in PLLA films. For the 1  $\mu\text{m}$  pitch samples, groove

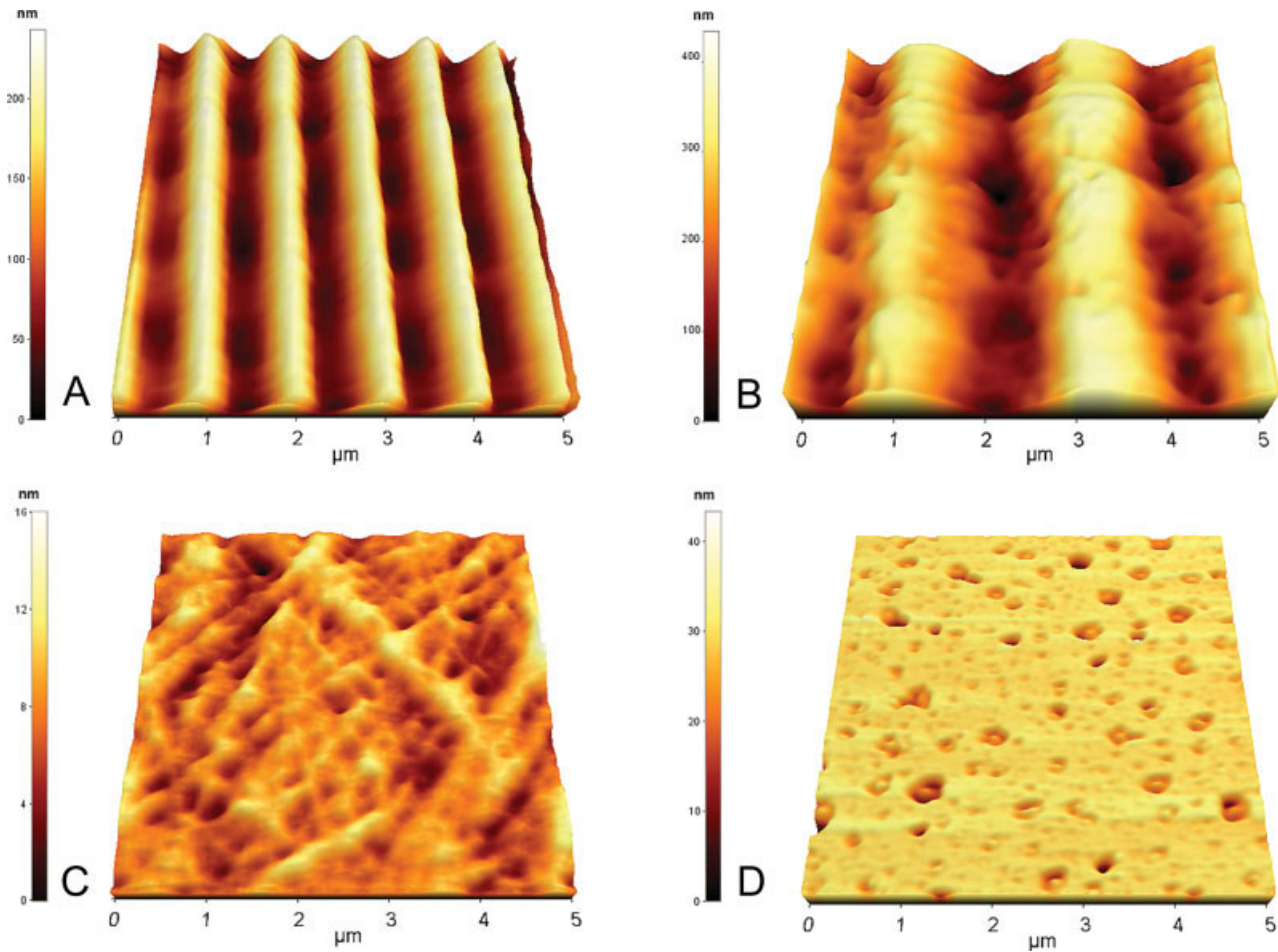


**Figure 2.** A: Atomic force microscope images of the patterned PLLA with 1  $\mu\text{m}$  spaced grooves. The image was disproportionately scaled in the z-direction to enhance surface features. Unidirectional grooves were sinusoidal in shape and had groove heights ranging from 100–180 nm. B: 2  $\mu\text{m}$  samples possessed moderately higher peak to valley values of 120–300 nm and slight roughness along the grooves. C: TCPS controls were quite smooth, although slight ridges and bumps were seen. D: PLLA controls were relatively flat with some nanoscale pores present. Nonetheless, average surface roughness ( $R_a$ ) still remained under 4 nm.

heights ranged from 100 to 180 nm with the average height being approximately 150 nm (Table I). The 2  $\mu\text{m}$  pitch specimens yielded heights in the 120–300 nm range, with a mean height of 215 nm. Topographical data taken from control TCPS showed a more level surface, although nanometer sized bumps and ridges were noticeable. Similar to patterned PLLA films, the PLLA controls exhibited sub-micron pores a few nanometers in height. However, both TCPS and PLLA controls were relatively smooth and devoid of

consistent directional features when compared with patterned counterparts.

**XPS**

XPS is a surface sensitive analytical technique that reports elemental composition to depths of approximately 10 nm. The XPS wide spectra of control and patterned PLLA films communicate comparable sur-

**TABLE I**  
Summary of Experimental Treatments

Treatment	Groove Spacing	Groove Height (avg)	Material	Tested Cell Type
Patterned	1 $\mu\text{m}$	150 nm	PLLA	PC-12, sympathetics
Patterned	2 $\mu\text{m}$	215 nm	PLLA	PC-12, sympathetics
Control	–	–	PLLA	PC-12, sympathetics
Control	–	–	TCPS	PC-12, sympathetics

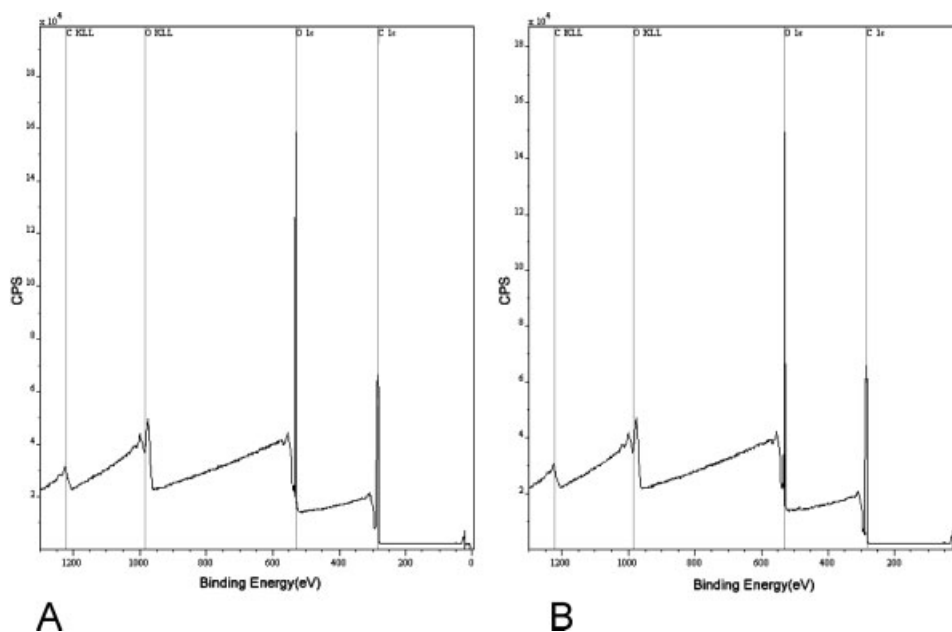


**Figure 3.** XPS wide spectrum of control (A) and patterned PLLA films (B). The spectrum consists of the characteristic peaks for carbon (284.5 eV) and oxygen (531 eV). The chemical composition based on the peak areal components was found to be 66.0% carbon and 34.0% oxygen for the control and 66.2% carbon and 33.8% oxygen for the patterned films. Other elements from contamination or residual solvent were not detected.

face chemistry (Fig. 3). For PLLA, the XPS spectrum contains peaks for carbon (284.5 eV) and oxygen (531 eV). Elemental fraction was found by integration of the region under the elemental peaks. Results for the controls were found to be 66.0% carbon and 34.0% oxygen while the patterned films were 66.2% carbon and 33.8% oxygen. Trace elements emanating from potential surface contaminants or residual chloroform solvent were negligible.

### Neurite alignment

Phase contrast images of PC-12 cells cultured onto respective substrates are shown in Figure 4. It is clearly evident that both polystyrene [Fig. 4(A)] and PLLA controls [Fig. 4(B)] showed similar neurite outgrowth characteristics. As expected, neurite emergence and neurite angles were uniformly distributed over the entire range of angles (expected value = 0.167) for both TCPS and PLLA controls (Fig. 5). However, in the substrates possessing topography, the PC-12 cells exhibited 54% and 47% parallel neurite alignment for 1 and 2  $\mu\text{m}$  periodicity, respectively. The neurites also emerged from the soma in a nonuniform manner, with a biased proportion of neurites emanating within  $15^\circ$  of the groove direction (40% for 1  $\mu\text{m}$ , 37% for 2  $\mu\text{m}$ ). Cells also exhibited turning behavior shortly after emergence from cell body.

Sympathetic neurons also followed classical parallel contact guidance comparable to PC-12 cells (Fig. 4).

Again, neurite emergence and neurite orientation angles coincided with a uniform distribution in both TCPS and PLLA controls (Fig. 6). In the 1 and 2  $\mu\text{m}$  pitched grooves, the sympathetic neurons exhibited even greater directionality than PC-12s, with 72% and 46% parallel neurite alignment, respectively. Likewise, the neurites emerged from the soma with a higher frequency along the grooves, 44% and 34% for 1 and 2  $\mu\text{m}$ , respectively. For the subpopulation of neurites with parallel emergence and orientation angles ( $\alpha, \beta \leq 15^\circ$ ), statistical comparisons were made between groups of the same cell line. Differences in  $\beta$  angles were observed in PC-12 cells between the grooved substrata in addition to grooved vs. controls. No significance was observed for  $\alpha$  angles between grooved groups. With sympathetic neurons, differences in the emanation and orientation angles were seen between 1  $\mu\text{m}$  grooved and grooved vs. controls. Table II represents a summary of the statistical findings.

### Neurite lengths

In terms of neurite length, PC-12 cells plated onto grooved substrates did not show statistical deviations from controls (Fig. 7). However, sympathetic neurons displayed longer neurite lengths on the patterned substrata. Average neurite lengths ( $\pm$ S.E.) for the TCPS and PLLA controls were  $135.1 \pm 3.18 \mu\text{m}$  and  $134.4 \pm 2.94 \mu\text{m}$  while 1 and 2  $\mu\text{m}$  had lengths

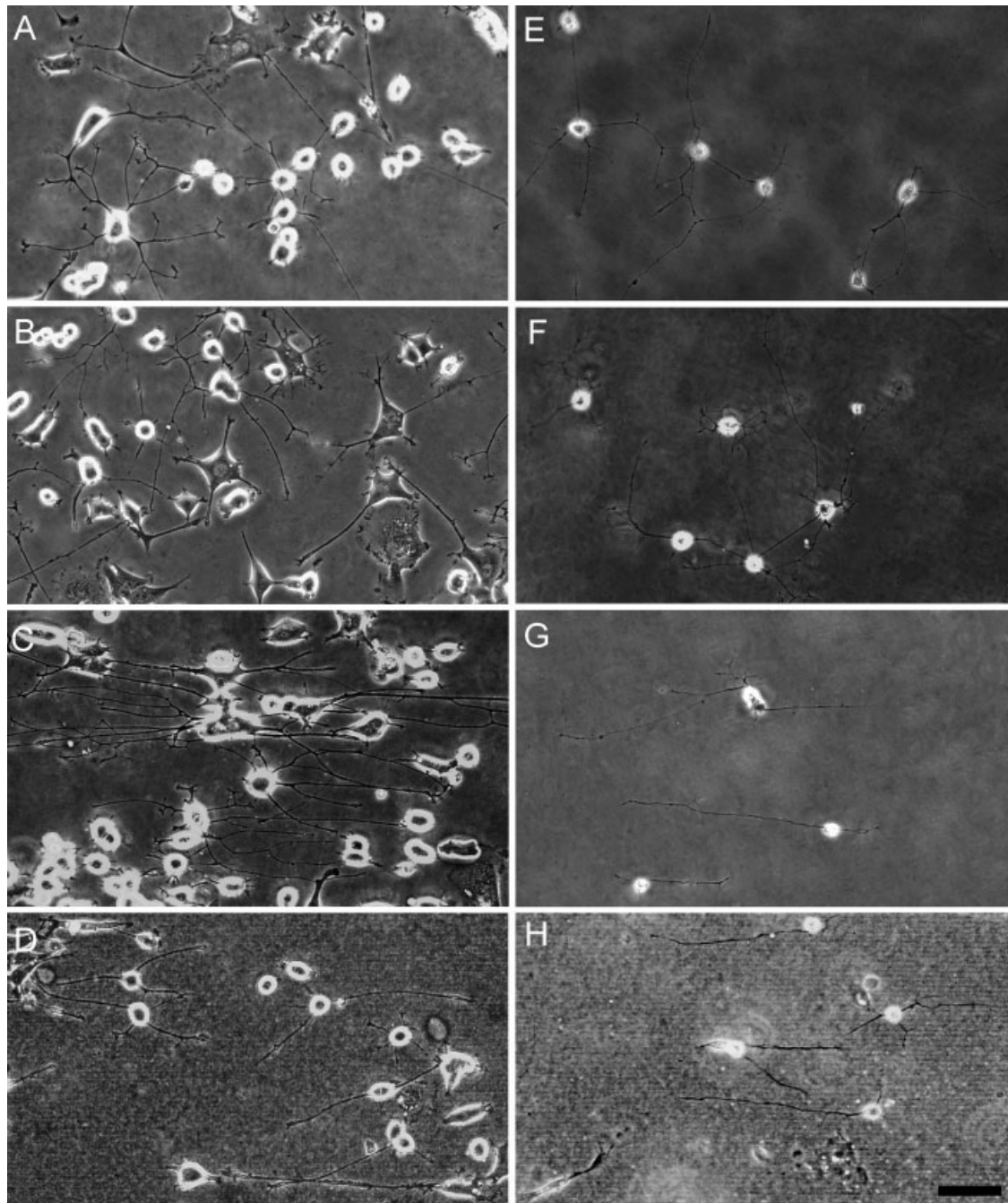


**Figure 4.** Typical phase contrast images of PC-12 cells cultured onto various surfaces after 48 h of NGF supplemented media (A)–(D). A: TCPS control. B: PLLA control. C: Cells on 1  $\mu\text{m}$  PLLA films and (D) PC-12 on 2  $\mu\text{m}$  PLLA substrates (horizontal direction is the direction of underlying grooves). Phase contrast image of chick sympathetic neurons cultured onto various surfaces after 24 h of incubation (E)–(H). E: TCPS control. F: PLLA control. G: Cells on 1  $\mu\text{m}$  PLLA. H: Sympathetics on 2  $\mu\text{m}$  PLLA. Scale bar: 50  $\mu\text{m}$  (A)–(H).

of  $177.5 \pm 5.88 \mu\text{m}$  and  $152.7 \pm 4.03 \mu\text{m}$ , respectively.

#### Cell architecture

Cellular complexity was used to address the possibility that surface contours may dictate the number of

formed neurites or extent of neural arborization. Although data on TCPS was characterized, TCPS served as a reference and statistical comparisons were only made between PLLA surfaces. This approach was taken to eliminate confounding effects of substratum material and topography. Quantitative analysis of cell architecture showed PC-12 cells were not influenced by surface patterning. This observation was



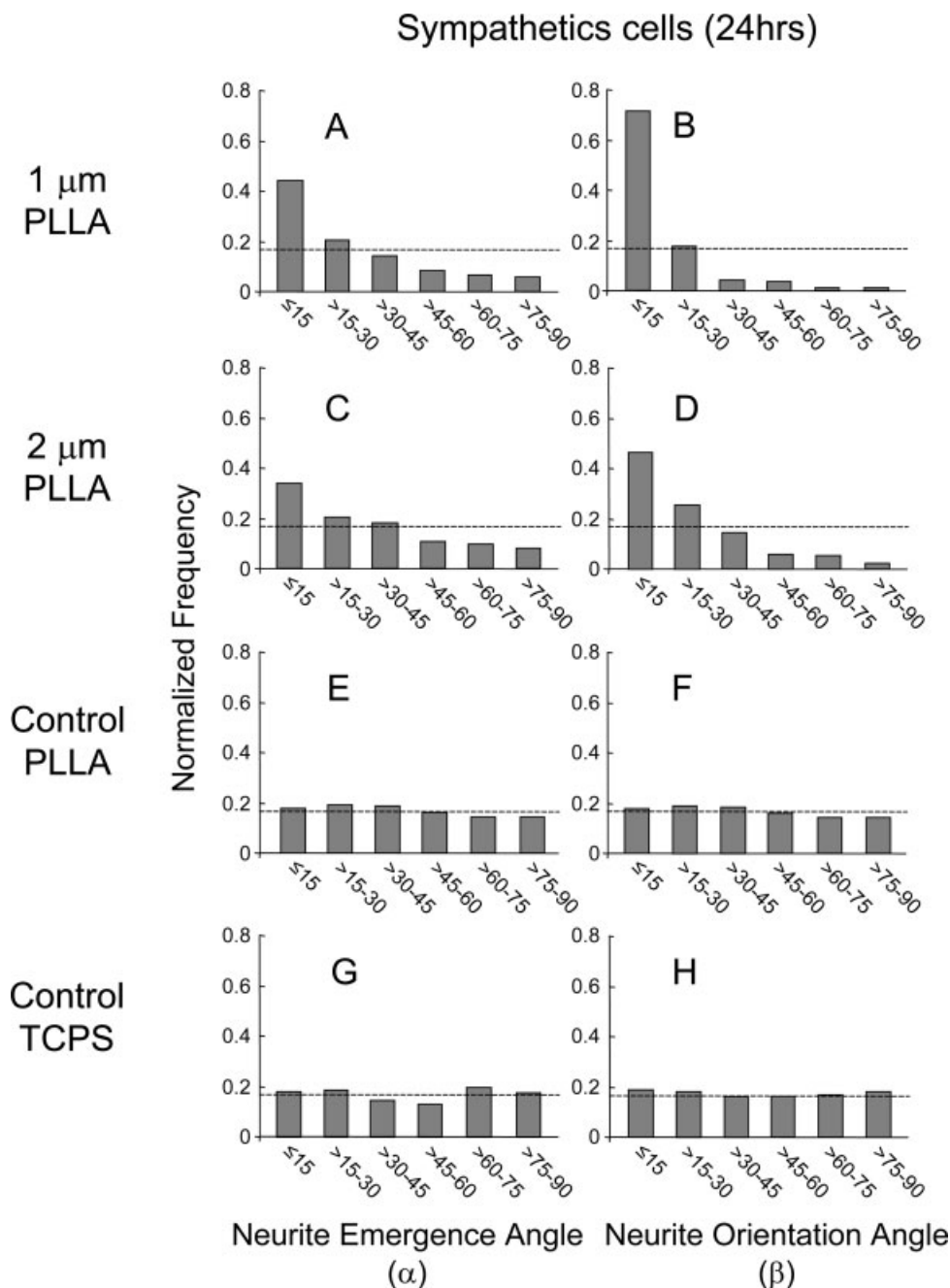


**Figure 6.** Histograms of neurite emergence angle and the neurite orientation angle for chick sympathetics ( $n = 400-900$  per condition). Again, neurite emergence and neurite angles are uniformly distributed (dashed line represents expected value of 0.167) for both TCPS and PLLA controls. In contrast, sympathetics on 1 and 2  $\mu\text{m}$  surfaces exhibited 72% and 48% parallel alignment, respectively. Neurites also emerged from the soma within a preferred range of angles.

ing properties. Since the polymer substratum is thin and soft, the neurons may have contorted and deformed the substrates. This was evident in some of the SEM micrographs, where impressions within the substratum were seen (Fig. 9). Moreover, higher magnifications of neural processes revealed distinct attachment points to the substrate [Fig. 9(A,E)]. Inspection of neurite alignment showed that in some cases of parallel orientation, the neurites were

guided by the grooves and were able to conform to the groove channels [Fig. 9(B,D)]. This is not surprising since 1–2  $\mu\text{m}$  is approximately the size of most neurite shafts within our culture system. However, in other instances of parallel alignment, the neurites spanned several grooves and conformation to the substrate was not seen [Fig. 9(A,C)]. This was especially prominent in the 1  $\mu\text{m}$  PLLA substrates. Numerous filopodia were seen extending outwards

**TABLE II**  
**Statistical Significance Matrix for Parallel Neurite**  
**Cases ( $\alpha, \beta \leq 15^\circ$ )**

	1 $\mu\text{m}$ PLLA	2 $\mu\text{m}$ PLLA	Control PLLA	Control TCPS
PC-12 cells				
1 $\mu\text{m}$ PLLA		$\beta/+^*$	$\beta/+^*$	$\beta/+^*$
2 $\mu\text{m}$ PLLA	$\alpha/-$		$\beta/+^*$	$\beta/+^*$
Control PLLA	$\alpha/+^*$	$\alpha/+^*$		$\beta/-$
Control TCPS	$\alpha/+^*$	$\alpha/+^*$	$\alpha/-$	
Sympathetics cells				
1 $\mu\text{m}$ PLLA		$\beta/+^*$	$\beta/+^*$	$\beta/+^*$
2 $\mu\text{m}$ PLLA	$\alpha/+^*$		$\beta/+^*$	$\beta/+^*$
Control PLLA	$\alpha/+^*$	$\alpha/+^*$		$\beta/-$
Control TCPS	$\alpha/+^*$	$\alpha/+^*$	$\alpha/-$	

$\alpha/$ , denotes  $\alpha$  angle comparisons;  $\beta/$ , denotes  $\beta$  angle comparisons; +, significant; -, insignificant.

\* $p < 0.05$ .

at the growth cones of sympathetic neurons [Fig. 9(E)]. In rare cases where the neurite grew perpendicular to the grooves, it was observed that a significant number of attachment points were formed solely at groove ridges [Fig. 9(E)].

## DISCUSSION

The cellular response to topographical features represents a well-established phenomenon. Topology has been implicated in processes such as migration and early development.<sup>11–15</sup> Nordlander et al. (1991) also found that growth cones often aligned with other neurites during regeneration.<sup>12</sup> Further, fibroblasts, smooth muscle, Schwann cells, and osteoblasts also respond to topography through increased attachment, alignment, up-regulated protein synthesis or enhanced bone deposition.<sup>23–28</sup> Even more interesting is that cells show improved function to geometric features in the nanoscale regime as opposed to micron topographies.<sup>24,26–28</sup> We therefore hypothesized that submicron dimensioned topologies would be a suitable size scale to enhance neural pathfinding. Although seminal topographical studies with neurons have been carried out using traditional photolithographic techniques, the surface features were commonly etched onto materials not necessarily desirable for *in vivo* application. Additionally, it is well known that cells react differently to parameters such as wettability, compliance, surface free energy, and charge.<sup>20,21</sup>

The rationale for the present study was to therefore determine whether previous cellular responses to hard surfaces could be translated to easily deformable, degradable PLLA films. This is a necessary step in evaluating the potential of soft topography-based strategies for clinical usage. PLLA was chosen

for its degradable nature and application in wide ranging biomedical fields. With a solvent casting process, we fabricated films of approximately 20  $\mu\text{m}$  thick with continuously repeating grooves of 1 and 2  $\mu\text{m}$  pitch and height features approaching the nanoscale. Surface features imparted onto the PLLA emulated original acetate masters in terms of groove height and spatial frequency (data not shown). However, minor surface dimples (Fig. 2) were recorded with the AFM, which we attribute to nonuniform solvent evaporation.

The effects of topography were subsequently probed with PC-12 and chick sympathetic neurons as the model systems. The emphasis of the present study was on individual neurite characteristics, such as length and the extent of neurite alignment. Directionality was assessed with a dual parameter method (emanation and final orientation angle) to permit tracking of neurite trajectories. We also investigated neurite outgrowth by quantifying the degree of arborization as a function of soma distance. To mitigate the effects of neighboring cells on neurite character-

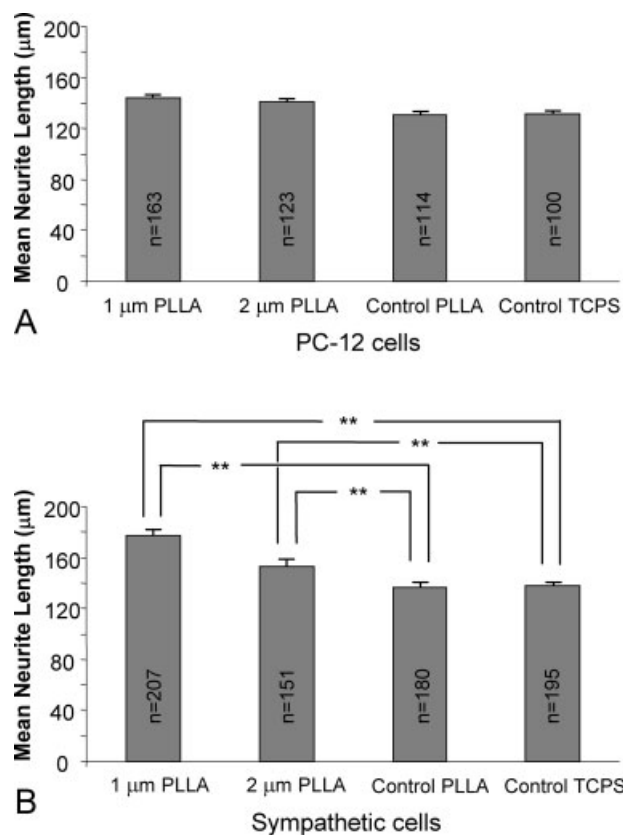


**Figure 7.** Mean neurite lengths ( $\pm$ SE) are presented for PC-12s (A) and chick sympathetic neurons (B). PC-12s seeded onto nanopopographical substrates did not show significant differences from controls while sympathetics on 1 and 2  $\mu\text{m}$  PLLA were statistically significant when compared with control (\*\* $p < 0.01$ ).

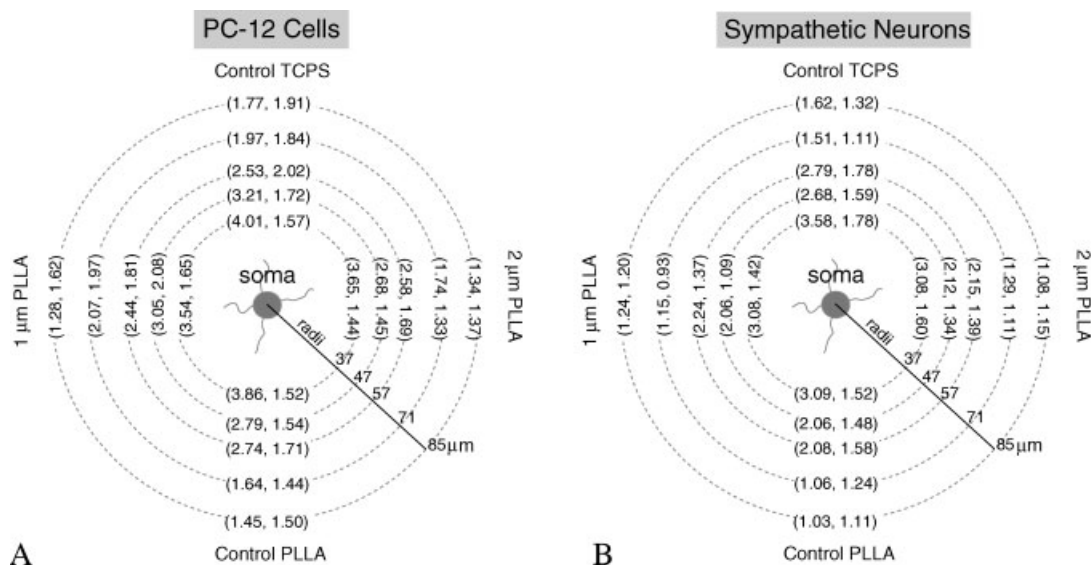


**Figure 8.** The average number of neurites and branching complexity were assessed as a function of distance from the soma. Data for PC-12 cells (A) and chick sympathetic neurons (B) are presented as (mean number of intersections, standard deviation). For each cell type, only statistical comparisons at each radius were made between PLLA cases. Results show PC-12 cells did not differ in neural complexity at all distances from the soma. Sympathetic neurons established on PLLA yielded similar results with no statistical differences observed. These findings therefore emphasize that on the same biomaterial, patterning had no effect on neural arborization.

istics, lower cell seeding densities were used and only neurites free from contact were quantified.

Our results convey that contact guidance in the form of repetitive sinusoidal grooves constitutes a simple and effective method for influencing cell response. Stereotyped emanation and orientation angles were salient, especially on 1 μm spaced substrata. The directional cues provided by the substrate also impacted the cell in an active manner with neural processes turning towards the direction of the underlying grooves. This turning response can be seen directly [Fig. 4(C,D)] and is implied via the population differences between emanation angles and eventual neurite alignment (Figs. 5 and 6). Neurite growth towards the substratum grooves was also apparent in previous studies of neural pathfinding.<sup>16,18,29</sup> SEM micrographs of growth cones further show multiple filopodia radiating in all directions [Fig. 9(E)]. Taken together, these findings confirm the notion that cells continually and actively survey the local microenvironment for directional cues.

The rate of neurite extension on grooved substrata was also increased, especially for sympathetic neurons, which displayed 10–30% longer neurites than controls. Comparable findings were found with *xenopus* spinal neurons and hippocampal neurons, which demonstrated enhanced growth on patterned glass.<sup>16</sup> In contrast, PC-12 cells did not generate longer neurites on grooved surfaces. This result may be attributed to cell lineage discrepancies as the PC-12 cells could have reached an optimum growth threshold that could not be exceeded with topographical stim-

uli. Although some trend differences were noted between PC-12 and sympathetic neurite lengths, no significant findings in the cell architecture were observed. Neither the number of neurites generated nor the degree of neuronal branching differed between patterned and unpatterned surfaces (Fig. 9). This emphasizes that with the current experimental model, unidirectional contours enhance neurite orientation and increases length but have no effect on cellular architecture. We should note that XPS data of PLLA verified surface conditions were similar for control and patterned films and suggests observed cellular differences to be based solely on topography and not via surface chemical or compositional differences arising from substrate manufacturing.

The mechanism of contact mediated guidance is still unclear. Directional constraint of the cell cytoskeleton has been proposed since repeating grooves may inhibit cytoskeletal polymerization in directions orthogonal to substratum grooves.<sup>30–33</sup> This conclusion is based on the property that cytoskeletal elements possess limited flexibility and contact with an obstruction, such as a channel wall could deter cytoskeletal formation. The stiffness associated with the cell membrane network would similarly tend to induce cell bridging of the grooves, confining cell adhesion to only ridge tops in cases of narrow ridge spacing.<sup>34</sup>

Indeed, we did observe slightly greater parallel alignment when the spatial periodicity was decreased to 1 μm. Certainly, groove depth may play a role, but since the height variations between 1 and

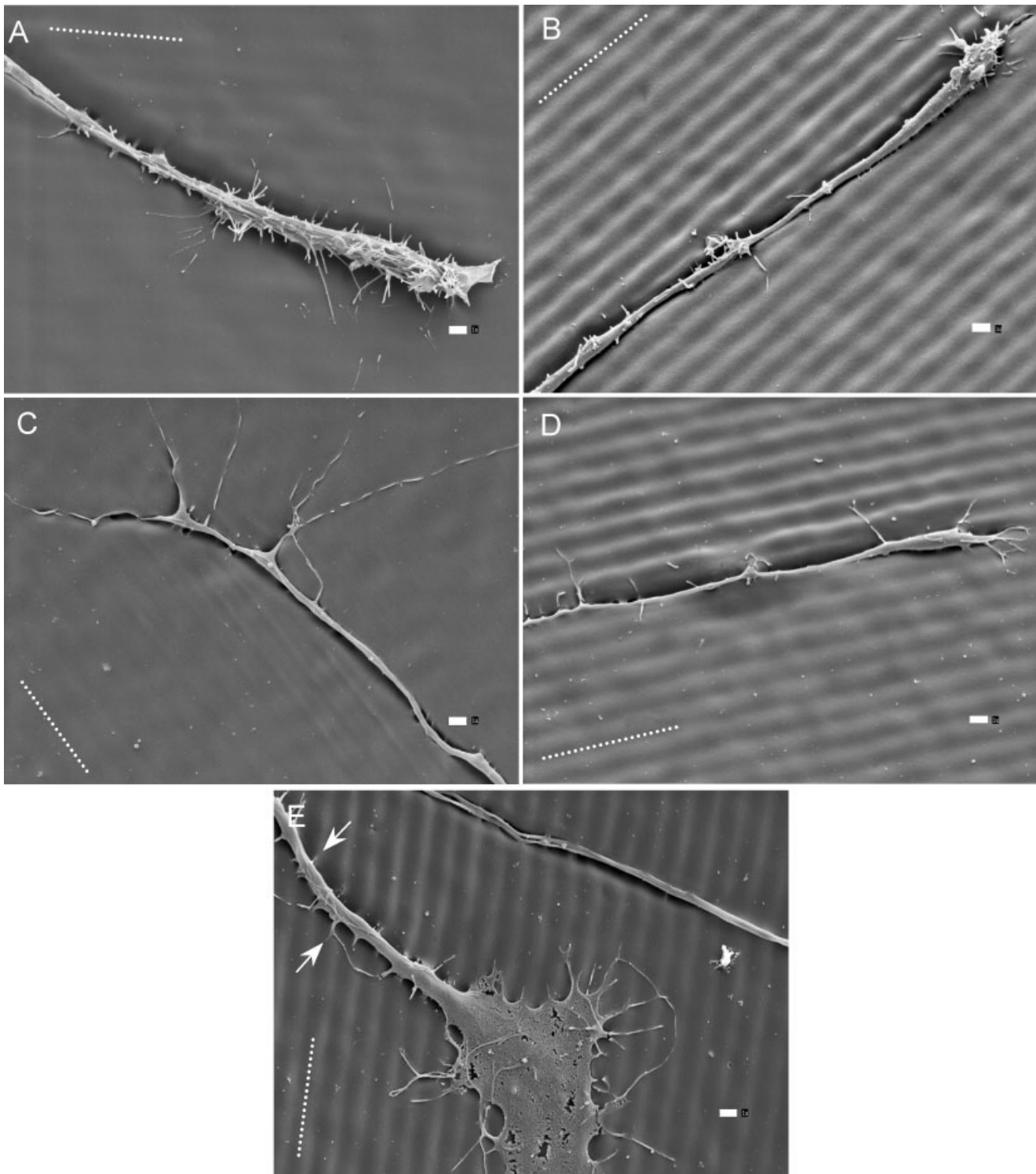


**Figure 9.** A: SEM micrographs of PC-12 cells ( $\times 4000$  magnification) growing on 1  $\mu\text{m}$  spaced PLLA film. For better visualization, long white dotted lines were superimposed on all images to highlight the direction of substratum grooves. Also in this micrograph, the cell membrane has torn away and the neurofilaments are clearly evident. B: SEM image of a PC-12 neurite on 2  $\mu\text{m}$  spaced PLLA. This particular neurite appears to be guided by the underlying topography, being conformed to the native channels. C: Sympathetic neurite on 1  $\mu\text{m}$  PLLA. D: Sympathetic neurons on 2  $\mu\text{m}$  spaced PLLA were similar to PC-12 cells, with neurites following the channel valleys. E: In rare cases where the neurite grew perpendicular to the grooves, a significant number of attachments (white arrows) to the groove ridges were noted. Shown is a sympathetic neurite and corresponding growth cone. White scale bar: 1  $\mu\text{m}$  (A)–(E).

2  $\mu\text{m}$  patterns were on average, less than 75 nm, we speculate the increased alignment on 1  $\mu\text{m}$  patterns to be due to higher groove frequency. In terms of ridge bridging, we only observed this behavior in a few instances. Perpendicular aligned neurites showed noticeable bridging behavior but parallel aligned neurites demonstrated a capacity to traverse across and into the channels (Fig. 9). At the wider groove spacing (2  $\mu\text{m}$ ), neurites were physically constrained by the channel walls, as evident in some of the SEM micrographs [Fig. 9(B,D)]. This phenomenon may be explained by the current substrate material and geometry. The PLLA films were relatively compliant, while the groove channels were shallow (<250 nm), wide (1–2  $\mu\text{m}$ ), and curved. These characteristics are in contrast to the rigid, stepped features of conventional micromachined substrates. Therefore, neurite bridging across the groove ridges may be less common with sinusoidally patterned grooves.

An alternate hypothesis for contact mediated guidance has been proposed by Ohara and Buck (1979) who suggested confinement of focal adhesions along groove ridges could control the overall cell shape.<sup>34</sup> Dunn and Brown (1986) believed that focal adhesions in the groove were less effective in allowing the cell to exert tractional forces necessary for migration.<sup>35</sup> Perhaps closely related is the possibility that serum or ECM proteins adsorb selectively on surfaces with controlled topography. Surface energy effects have been hypothesized to control protein patterning on topographical discontinuities or on surfaces exhibiting anisotropic composition.<sup>21,36</sup> This selective protein deposition has been shown to exist with micropatterned surfaces (but not nanopatterned) where laminin preferentially adsorbed to groove bottoms.<sup>25</sup> Since all substrata were pretreated with laminin, it is feasible that passive spatial patterning of laminin along groove ridges or troughs could facilitate pathfinding.

It is probable that the transduction of physical cues entails several competing mechanisms, whereby the influence of each mechanism is a function of the underlying topography. For instance, Rajnicek et al. (1997) found with rat hippocampal cells, either perpendicular or parallel alignment could be attained by merely altering groove dimensions.<sup>16,29</sup> Further, blocking actin formation with cytochalasin B did not eliminate perpendicular alignment behavior in hippocampal cells. Others have similarly concluded that focal adhesion and actin formation were not necessary for parallel alignment in fibroblasts and in human epithelial cells.<sup>33,37,38</sup> Perpendicular neurite alignment is especially interesting since this process cannot be explained by lateral cytoskeletal inhibition theories. Indeed these observations suggest the complexity of contact mediated guidance and the exist-

tence of several possibly distinct or synergistic mechanisms.

Physical guidance or topographical cues comprise one strategy for eliciting desired cell behavior. We believe that by studying guidance properties on materials most likely to be implanted, we can gain a more representative *in vivo* response. To our knowledge, this is the first attempt to investigate neural contact guidance with PLLA and surface grooves near the nanoscale. Neurite orientation effects compare favorably with other PC-12 studies on etched silicon<sup>39</sup> and mouse sympathetic neurons on polymethylmethacrylate.<sup>40</sup> Therefore, the mechanisms of contact mediated guidance seems to be well conserved across analogous cells of different species and on contrasting substratum materials. These results are encouraging for the implementation of soft lithographic processes for *in vivo* use.

## CONCLUSION

We have manufactured PLLA based polymer films possessing sinusoidal grooves of 1 and 2  $\mu\text{m}$  in width and 150 and 215 nm in average height, respectively. We show that when cultured onto these patterned films, PC-12 and chick sympathetic neurites emerged from the soma and align predominately in a direction parallel to the underlying grooves. Neurite lengths with chick sympathetic neurons were also longer compared with unpatterned controls. No apparent changes were seen in neurite arborization between patterned and unpatterned substrates. This exercise in topographical control has practical implications in tissue engineering and nerve repair. In situations involving nerve injury, nerve regeneration, and subsequent functional reconnection could be accelerated in the presence of well-controlled physical guidance. Guided regeneration can reduce neurite wandering or aberrant regeneration. In turn, these characteristics would mitigate the time delay between initial trauma and distal target reconnection. Further, a preferred cellular orientation may also benefit other fields of study including research with brain machine interfaces and artificial networks.

We acknowledge Judy Grimmer and Tracy Lui for assistance with cell culture.

## References

1. Tessier-Lavigne M, Goodman CS. The molecular biology of axon guidance. *Science* 1996;274:1123–1133.
2. Nieto MA. Molecular biology of axon guidance. *Neuron* 1996;17:1039–1048.

3. Keynes R, Cook GM. Axon guidance molecules. *Cell* 1995;83:161–169.
4. Adams DN, Kao EY, Hypolite CL, Distefano MD, Hu WS, Letourneau PC. Growth cones turn and migrate up an immobilized gradient of the laminin IKVAV peptide. *J Neurobiol* 2005;62:134–147.
5. Dertinger SK, Jiang X, Li Z, Murthy VN, Whitesides GM. Gradients of substrate-bound laminin orient axonal specification of neurons. *Proc Natl Acad Sci USA* 2002;99:12542–12547.
6. Borgens RB. Stimulation of neuronal regeneration and development by steady electrical fields. *Adv Neurol* 1988;47:547–564.
7. Borgens RB, Blight AR, McGinnis ME. Functional recovery after spinal cord hemisection in guinea pigs: The effects of applied electric fields. *J Comp Neurol* 1990;296:634–653.
8. McCaig CD, Rajniecek AM, Song B, Zhao M. Controlling cell behavior electrically: Current views and future potential. *Physiol Rev* 2005;85:943–978.
9. Rajniecek AM, Robinson KR, McCaig CD. The direction of neurite growth in a weak DC electric field depends on the substratum: Contributions of adhesivity and net surface charge. *Dev Biol* 1998;203:412–423.
10. Weiss L. Cell contact phenomena. *In Vitro* 1970;5:48–78.
11. Super H, Soriano E. The organization of the embryonic and early postnatal murine hippocampus. II. Development of entorhinal, commissural, and septal connections studied with the lipophilic tracer DiI. *J Comp Neurol* 1994;344:101–120.
12. Nordlander RH, Gazerro JW, Cook H. Growth cones and axon trajectories of a sensory pathway in the amphibian spinal cord. *J Comp Neurol* 1991;307:539–548.
13. Nordlander RH, Singer M. Spaces precede axons in *Xenopus* embryonic spinal cord. *Exp Neurol* 1982;75:221–228.
14. Bard JB, Higginson K. Fibroblast-collagen interactions in the formation of the secondary stroma of the chick cornea. *J Cell Biol* 1977;74:816–827.
15. Edgar D, Kenny S, Almond S, Murray P. Topography, stem cell behaviour, and organogenesis. *Pediatr Surg Int* 2004;20:737–740.
16. Rajniecek A, Britland S, McCaig C. Contact guidance of CNS neurites on grooved quartz: Influence of groove dimensions, neuronal age and cell type. *J Cell Sci* 1997;110(Part 23):2905–2913.
17. Dowell-Mesfin NM, Abdul-Karim MA, Turner AM, Schanz S, Craighead HG, Roysam B, Turner JN, Shain W. Topographically modified surfaces affect orientation and growth of hippocampal neurons. *J Neural Eng* 2004;1:78–90.
18. Stepien E, Stanis J, Korohoda W. Contact guidance of chick embryo neurons on single scratches in glass and on underlying aligned human skin fibroblasts. *Cell Biol Int* 1999;23:105–116.
19. Xia Y, Rogers JA, Paul KE, Whitesides GM. Unconventional methods for fabricating and patterning nanostructures. *Chem Rev* 1999;99:1823–1848.
20. Lim JY, Hansen JC, Siedlecki CA, Hengstebeck RW, Cheng J, Winograd N, Donahue HJ. Osteoblast adhesion on poly(L-lactic acid)/polystyrene demixed thin film blends: Effect of nanotopography, surface chemistry, and wettability. *Biomacromolecules* 2005;6:3319–3327.
21. den Braber ET, de Ruijter JE, Smits HT, Ginsel LA, von Recum AF, Jansen JA. Effect of parallel surface microgrooves and surface energy on cell growth. *J Biomed Mater Res* 1995;29:511–518.
22. Sholl DA. Dendritic organization in the neurons of the visual and motor cortices of the cat. *J Anat* 1953;87:387–406.
23. Curtis AS, Wilkinson CD. Reactions of cells to topography. *J Biomater Sci Polym Ed* 1998;9:1313–1329.
24. Kay S, Thapa A, Haberstroh KM, Webster TJ. Nanostructured polymer/nanophase ceramic composites enhance osteoblast and chondrocyte adhesion. *Tissue Eng* 2002;8:753–761.
25. Miller C, Shanks H, Witt A, Rutkowski G, Mallapragada S. Oriented Schwann cell growth on micropatterned biodegradable polymer substrates. *Biomaterials* 2001;22:1263–1269.
26. Thapa A, Miller DC, Webster TJ, Haberstroh KM. Nanostructured polymers enhance bladder smooth muscle cell function. *Biomaterials* 2003;24:2915–2926.
27. Thapa A, Webster TJ, Haberstroh KM. Polymers with nano-dimensional surface features enhance bladder smooth muscle cell adhesion. *J Biomed Mater Res A* 2003;67:1374–1383.
28. Miller DC, Thapa A, Haberstroh KM, Webster TJ. Endothelial and vascular smooth muscle cell function on poly(lactic-co-glycolic acid) with nano-structured surface features. *Biomaterials* 2004;25:53–61.
29. Rajniecek A, McCaig C. Guidance of CNS growth cones by substratum grooves and ridges: Effects of inhibitors of the cytoskeleton, calcium channels and signal transduction pathways. *J Cell Sci* 1997;110(Part 23):2915–2924.
30. Dunn GA, Heath JP. A new hypothesis of contact guidance in tissue cells. *Exp Cell Res* 1976;101:1–14.
31. Clark P, Connolly P, Curtis AS, Dow JA, Wilkinson CD. Topographical control of cell behaviour. I. Simple step cues. *Development* 1987;99:439–448.
32. Clark P, Connolly P, Curtis AS, Dow JA, Wilkinson CD. Topographical control of cell behaviour. II. Multiple grooved substrata. *Development* 1990;108:635–644.
33. Teixeira AI, Abrams GA, Bertics PJ, Murphy CJ, Nealey PF. Epithelial contact guidance on well-defined micro- and nano-structured substrates. *J Cell Sci* 2003;116:1881–1892.
34. Ohara PT, Buck RC. Contact guidance in vitro. A light, transmission, and scanning electron microscopic study. *Exp Cell Res* 1979;121:235–249.
35. Dunn GA, Brown AF. Alignment of fibroblasts on grooved surfaces described by a simple geometric transformation. *J Cell Sci* 1986;83:313–340.
36. von Recum AF, van Kooten TG. The influence of microtopography on cellular response and the implications for silicone implants. *J Biomater Sci Polym Ed* 1995;7:181–198.
37. Wojciak-Stothard B, Curtis AS, Monaghan W, McGrath M, Sommer I, Wilkinson CD. Role of the cytoskeleton in the reaction of fibroblasts to multiple grooved substrata. *Cell Motil Cytoskeleton* 1995;31:147–158.
38. Oakley C, Brunette DM. Topographic compensation: Guidance and directed locomotion of fibroblasts on grooved micromachined substrata in the absence of microtubules. *Cell Motil Cytoskeleton* 1995;31:45–58.
39. Foley JD, Grunwald EW, Nealey PF, Murphy CJ. Cooperative modulation of neuritegenesis by PC12 cells by topography and nerve growth factor. *Biomaterials* 2005;26:3639–3644.
40. Johansson F, Carlberg P, Danielsen N, Montelius L, Kanje M. Axonal outgrowth on nano-imprinted patterns. *Biomaterials* 2006;27:1251–1258.